

Explosions of Xenon Clusters in Ultraintense Femtosecond X-Ray Pulses from the LCLS Free Electron Laser

H. Thomas,¹ A. Helal,¹ K. Hoffmann,¹ N. Kandadai,¹ J. Keto,¹ J. Andreasson,^{2,3} B. Iwan,^{2,3} M. Seibert,^{2,3} N. Timneanu,^{2,3} J. Hajdu,^{2,3} M. Adolph,⁴ T. Gorkhover,⁴ D. Rupp,⁴ S. Schorb,⁴ T. Möller,⁴ G. Doumy,⁵ L. F. DiMauro,⁵ M. Hoener,⁷ B. Murphy,⁷ N. Berrah,⁷ M. Messerschmidt,⁶ J. Bozek,⁶ C. Bostedt,⁶ and T. Ditmire^{1,*}

¹*Texas Center for High Intensity Laser Science, University of Texas, Austin, Texas 78712, USA*

²*Uppsala University, Uppsala, Sweden*

³*Stanford University, Menlo Park, California 94025, USA*

⁴*Institut für Optik und Atomare Physik, Technische Universität Berlin, 10623 Berlin, Germany*

⁵*Department of Physics, The Ohio State University, Columbus, Ohio 43210, USA*

⁶*LCLS, Stanford Linear Accelerator Center, Menlo Park, California 94025, USA*

⁷*Department of Physics, Western Michigan University, Kalamazoo, Michigan 49008, USA*

(Received 23 March 2011; revised manuscript received 21 October 2011; published 28 March 2012)

Explosions of large Xe clusters ($\langle N \rangle \sim 11\,000$) irradiated by femtosecond pulses of 850 eV x-ray photons focused to an intensity of up to 10^{17} W/cm² from the Linac Coherent Light Source were investigated experimentally. Measurements of ion charge-state distributions and energy spectra exhibit strong evidence for the formation of a Xe nanoplasma in the intense x-ray pulse. This x-ray produced Xe nanoplasma is accompanied by a three-body recombination and hydrodynamic expansion. These experimental results appear to be consistent with a model in which a spherically exploding nanoplasma is formed inside the Xe cluster and where the plasma temperature is determined by photoionization heating.

DOI: [10.1103/PhysRevLett.108.133401](https://doi.org/10.1103/PhysRevLett.108.133401)

PACS numbers: 36.40.-c, 32.80.Fb, 32.80.Rm

The Linac Coherent Light Source (LCLS) x-ray, free-electron laser permits the study of interactions of matter with femtosecond x-ray pulses at an intensity beyond 10^{16} W/cm². Understanding these interactions is crucial for future experiments involving the imaging of biological molecules, protein nanocrystals, DNA, or viruses. van der Waals clusters in the gas phase represent an ideal test bed for investigating the fragmentation physics of molecular systems in intense x-rays because no energy can be exchanged with a surrounding medium, and the interaction of high-intensity, near-infrared light with these atomic systems is widely understood [1,2]. The interaction of high-intensity extreme UV pulses with Xe clusters has been investigated in recent years at a photon energy of 90 eV and intensities up to 6×10^{14} W/cm² at the free-electron laser in Hamburg (FLASH) and have been reported in a series of publications [3–8]. However, only with the activation of the LCLS have such studies in the x-ray regime at photon energies near or above 1 keV become possible.

The physics of cluster explosions under intense, femtosecond extreme UV or x-ray irradiation is rather different than explosions driven by IR pulses. During the early stages of a cluster's irradiation by an intense short wavelength pulse, electrons are generated by single photon photoionization and by Auger emission following each inner shell photoionization event. Electrons exit the cluster, successively building up a positive charge in the cluster until the space-charge potential confines electrons

subsequently liberated. A charged layer of ions forms at the surface of the cluster while a quasineutral, inner plasma core fills in the center of the cluster [9]. Even though the pulses can be intense, the short wavelength results in a rather low ponderomotive force which cannot significantly perturb this inner plasma core. As a result, many of the processes of a plasma in local thermodynamic equilibrium such as recombination and charge exchange can occur. The fragmentation of the cluster happens in two steps after the x-ray pulse strikes the cluster. First, the outer charged layer of the cluster explodes, propelled by the repulsive Coulomb force between the ions. This is followed by a hydrodynamic expansion of the remaining charge-neutral plasma which is driven by the pressure of the electrons, resulting in the emission of ions with an energy spectrum reflecting the electron temperature [10].

In this Letter, we report experimental studies of these cluster explosion dynamics in large Xe clusters ($\langle N \rangle \sim 11\,000$) irradiated by intense x-ray pulses from the LCLS. We studied explosions of clusters in laser pulses of 850 eV photons with a pulse duration of 150 fs and peak intensity spanning from 4×10^{14} up to 6×10^{16} W/cm². We find that the maximum charge state Xe²⁶⁺ produced in Xe clusters at the highest intensities is virtually identical to the highest charge state observed when single Xe atoms are irradiated under identical conditions. On the other hand, photoionization of Xe clusters produces a large number of Xe⁺ and Xe²⁺, charge states virtually absent in the ion charge-state spectra of single Xe atoms irradiated under

identical conditions. We also observe that the distribution function of ion kinetic energies exhibits a shape characteristic of a plasma which has expanded hydrodynamically. These results are consistent with a model in which the LCLS laser pulse strips the Xe cluster atoms sequentially by photoionization and Auger emission to high charge states forming a nanoplasma whose temperature is determined by the photo- and Auger-electron energies, a process which can be described as “photoionization heating.” The formation of this nanoplasma leads to rapid three-body recombination during a hydrodynamic explosion of the inner core.

The experiment was conducted at the atomic molecular optical (AMO) physics beamline at the LCLS. The x rays were focused by a Kirkpatrick-Baez mirror configuration to an area of $2 \mu\text{m}^2$ [11]. The average energy per laser pulse was 1.1 mJ and the corresponding maximum intensity was $5.6 \times 10^{16} \text{ W/cm}^2$. A McLaren-type time-of-flight (TOF) spectrometer employing a multi-channel-plate detector detected the ions generated by the interaction of the light pulse with the cluster and atomic beams. A supersonic Xe gas expansion through a conical nozzle with a $100 \mu\text{m}$ diameter and a 15° cone angle generated the clusters. This process leads to a statistical size distribution around the mean cluster size [12]. To generate Xe clusters with a mean size of 10 000 atoms, a gas pressure of 8.2 bar at 300 K was expanded through the nozzle [12]. We used a pulsed General Valve nozzle with 2 ms pulse opening time to approach a steady-state flow during the gas pulse while still maintaining a pressure of less than 10^{-5} mbar in the source chamber. A $200 \mu\text{m}$ skimmer was installed 20 cm from the nozzle between the AMO source chamber and x-ray interaction chamber to reduce the atomic background there ($P < 10^{-7}$ mbar).

The ion-TOF spectra produced by the x-ray pulses over a range of intensities are illustrated in the first three panels of Fig. 1 while the fourth panel presents the ion-TOF spectrum from the irradiation of single Xe atoms at intensity of $5.6 \times 10^{16} \text{ W/cm}^2$. These spectra have been averaged over several thousand single LCLS pulses and result from an effective integration over clusters irradiated in a range of intensities in the Gaussian focus [11]. The ion charge-state spectra obtained from a Xe atomic source [Fig. 1(d)] are well explained by sequential ionization by the large x-ray fluence. No Xe^+ and almost no Xe^{2+} or Xe^{3+} are visible in this spectrum, while charge states up to $26+$ are clearly visible. The dearth of the signal in the $1+$, $2+$, and $3+$ peaks reflects an Auger cascade resulting from the $3d$ -innershell ejection; the first photoionization event leads to the removal of a $3d$ electron most of the time, which is immediately followed with very high probability by an Auger emission of 3 or 4 additional electrons [13]. Subsequent photoionization strips the Xe atoms to higher charge states until the x rays can no longer remove electrons by single photon absorption, which occurs once the

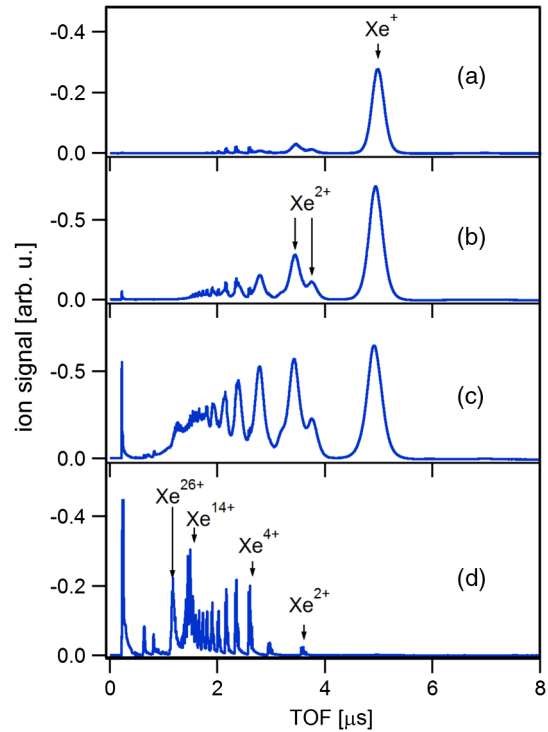


FIG. 1 (color online). Ion-TOF spectra for 150 fs pulse length and 850 eV photon energy. (a) Xe clusters $\langle N \rangle = 11\,000$, Intensity = $5.6 \times 10^{14} \text{ W/cm}^2$. (b) Xe clusters $\langle N \rangle = 11\,000$, Intensity = $5.6 \times 10^{15} \text{ W/cm}^2$. (c) Xe clusters $\langle N \rangle = 11\,000$, Intensity = $4.5 \times 10^{16} \text{ W/cm}^2$. (d) Xe atom Intensity = $5.6 \times 10^{16} \text{ W/cm}^2$.

Xe atom reaches $26+$ (since the energy needed to ionize Xe^{26+} to Xe^{27+} is $\sim 1440 \text{ eV}$).

In contrast, the cluster ion spectra of Fig. 1 differ significantly from the spectra resulting from Xe atoms. These cluster-produced ions show a significant number of Xe^+ , Xe^{2+} , and Xe^{3+} ions; in fact, an estimated 80% of the total integrated ion signal comes from charge states Xe^{1+} to Xe^{6+} even at the highest investigated intensity. Xe^+ is by far the most likely ion in clusters, while being completely absent in Xe atoms. This behavior can be explained if a Xe nanoplasma forms and lower charge states are produced by three-body recombination in the dense Xe plasma.

A close-up of ion-TOF spectra generated by intensities from 4.5×10^{14} to $5.6 \times 10^{16} \text{ W/cm}^2$ is displayed in Fig. 2 for selected charge states between Xe^+ and Xe^{6+} . First, for our jet parameters there are isolated Xe atoms remaining in the cluster beam. The contribution to the TOF spectrum from these atoms leads to a series of sharp peaks, each resulting from a different Xe isotope (absent, as already noted in the $1+$ feature). These ions are produced with essentially zero initial kinetic energy and arrive at flight times that correspond to this zero initial energy for each charge. For clarity, the zero kinetic energy time from isolated atoms is marked with a gray bar in Fig. 2. The other two contributors to the TOF spectrum of each charge

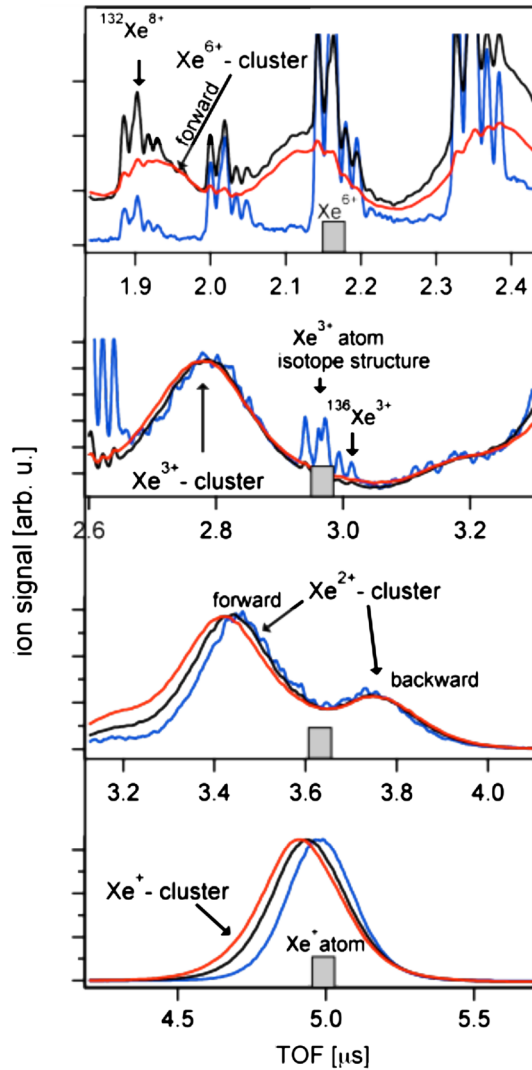


FIG. 2 (color online). Intensity-dependent ion-TOF spectra from Xe clusters with $\langle N \rangle = 10000$ for select charge states Xe^+ to Xe^{6+} . X-ray pulse intensities are $4.5 \times 10^{14} \text{ W/cm}^2$ (lower trace, blue), $4.5 \times 10^{15} \text{ W/cm}^2$ (upper trace, black), and $5.6 \times 10^{16} \text{ W/cm}^2$ (middle trace, red). The gray bars show the ion positions for atomic photoionization.

state are ions ejected from clusters along the axis of the TOF tube toward the detector, which arrive earlier than the zero kinetic energy time, and ions ejected away from the detector, which arrive later. (A small slit aperture of $2 \text{ mm} \times 0.2 \text{ mm}$ rejects most ions ejected in a direction perpendicular to the TOF flight axis.) The magnitude of this forward-backward peak splitting is an indication of the magnitude of the energy of the ejected ion. The important observation from Fig. 2 is that the peak splitting is virtually independent of x-ray pulse intensity. The average kinetic energy, for example, of Xe^{6+} was $\sim 1.2 \text{ keV}$.

Further information about the explosions of the Xe clusters was derived by examining the ion spectra when the extraction grid voltages were removed, which yielded TOF traces in which the ion flight time is determined directly by

the energy each ion acquires in the cluster's explosion. This technique allows us to measure the Xe ion-energy spectrum directly. An example of an ion-energy spectrum from the Xe clusters is illustrated in Fig. 3(a). Using a standard model for hydrodynamic expansion of a Xe plasma [14], we find that this spectrum is well described by that expected from a hydrodynamic expansion, a characteristic spectrum well documented in the explosion of Xe clusters irradiated by intense, near-infrared laser pulses [10]. The fit for a hydrodynamic expansion for a Xe plasma with an initial electron temperature of 125 eV is illustrated in Fig. 3(a) and matches the observed ion spectrum very well. In this calculation, we assumed a mean charge $\langle q \rangle = +5$ for the plasma, which we determined from an average over the observed charge-state distribution reproduced in Fig. 1.

In this experiment, we also acquired electron energy spectra from electron TOF spectrometers in the LCLS AMO chamber. An example of these data is illustrated in Fig. 4 (bottom panel). The photoelectron peaks from 3d

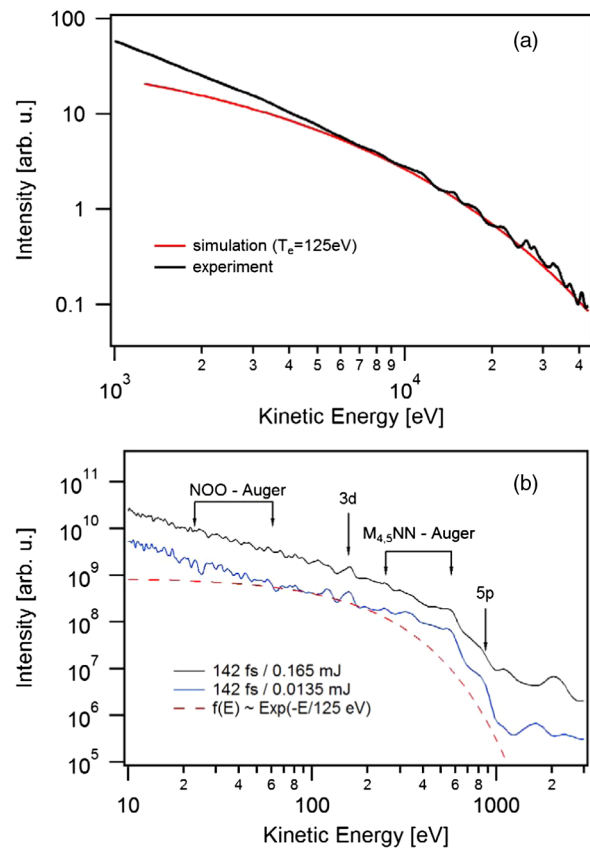


FIG. 3 (color online). (a) Measured Xe ion-energy spectrum from exploding Xe clusters at intensity $5.6 \times 10^{16} \text{ W/cm}^2$ from the field-free drift measurement. A hydrodynamic simulation of the ion-energy spectrum assuming a mean electron temperature of $\sim 125 \text{ eV}$ is shown for comparison with the experimental ion drift measurement. (b) Kinetic electron spectra from Xe clusters for two different pulse energies at a pulse length of 142 fs. The distribution function for a 125 eV Maxwellian function is shown as a dashed line.

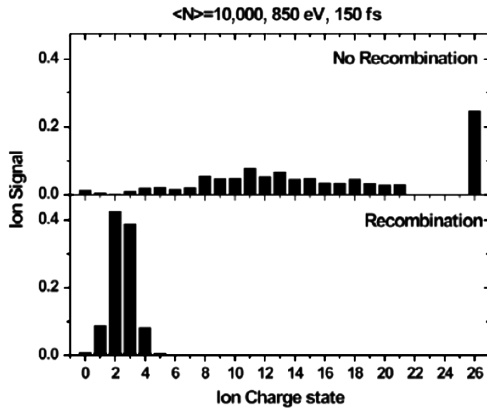


FIG. 4. Rate equation calculation of the charge distribution from the irradiation of 10 000 atom Xe clusters by 150 fs, 850 eV x-ray pulses at intensity 5×10^{16} W/cm². The top shows when no recombination is included and the bottom shows the inclusion of recombination.

and $5s/5p$ photoionization and Auger electrons emitted in the range from 340–630 eV [15] are all visible in this electron energy spectrum, which is dominated by a broad, thermal distribution. A Maxwellian with an electron temperature of 125 eV is reproduced in this figure, which compares well with the thermal distribution observed in the data.

All of these data suggest that a dense nanoplasma is formed in the x-ray pulse and that this plasma expands by hydrodynamic forces. The electron temperature of this residual space-charge confined plasma is near 125 eV. At this temperature and cluster size, less than 1% of the electrons can escape from the cluster (with a mean charge of 5+). Consequently, the presence of low Xe charge states is easily explained by rapid three-body recombination of the higher Auger-produced charges. One possible explanation for the observed temperature is that the electron fluid energy is essentially determined by the residual energy of the photoionized and Auger ejected electrons thermalized by rapid electron collisions, a process that might be called photoionization heating.

To gain insight into this process and confirm this explanation, we created a simple rate equation model along the lines of that first presented in Ref. [16]. This model calculated the production of charge states during the x-ray pulse interaction with the Xe cluster solving rate equations using photoionization cross sections and dominant Auger-electron emission pathways. From known x-ray cross sections, an 850 eV photon excites a $3d$ electron of a neutral Xe atom with 83% probability, and $4d$, $4p$, and $5p$ electrons with 9.4%, 5.2%, and 0.8% probability, respectively [17]. We therefore assume that all initial photoionization events are $3d$ ejections followed by the most probable Auger cascades which eject three or four additional electrons with energies ranging from about 430 to 20 eV [13,18,19]. The $3d$ photoionization remains the dominant

ionization process until the ionization potential of $3d$ electrons is higher than the photon energy, which is the case at about Xe^{10+} - Xe^{12+} depending on the electron density of the nanoplasma, which lowers the ionization potential. From these rates and ejected electron kinetic energies, the electron temperature was determined, combined with cooling from adiabatic expansion of the spherical Xe cluster plasma and evaporating electron cooling. The time history of the Xe charge states was calculated from ionization with the additional effects of three-body recombination and collisional ionization. We conclude from this simulation that the Xe cluster core does not significantly expand during the ~ 150 fs x-ray pulse and that the rate of recombination in this solid density plasma is significant.

Figure 4 shows the predicted charge-state distribution from the expanded Xe cluster. The top panel illustrates our calculation when recombination is turned off (essentially approximating the dynamics of single Xe atom ionization), and at the bottom when recombination in the Xe cluster is correctly included. When recombination is neglected we find that sequential ionization essentially strips the Xe ions to 26+ with very little ion production between 1+ and 6+. This roughly approximates the charge-state distribution observed in single Xe atoms when it is recalled that the actual experiment is performed in a focal spot with a range of intensities that lead to more Xe ion production at charges below 26+. When recombination is included along with the electron temperature dynamics described above, the predicted electron temperature is around 150 eV, remarkably close to that found from the hydrodynamic fit to the Xe ion-energy spectra and almost all Xe ions have charges between 1+ and 4+, which is qualitatively consistent with the data. We note that our model does not seem to predict the continued presence of high charge states in the Xe charge-state spectrum. This could be a result of the fact that our model does not account for the Coulomb explosion of the shell of ions around the quasineutral nanoplasma core that are not expected to undergo recombination.

In conclusion, we have observed the explosion of large Xe clusters subject to irradiation by intense laser pulses of 850 eV photons from the LCLS. The presence of low charge states, the lack of significant variation in ion-energy with incident intensity, the observed shape of the Xe ion-energy spectrum and the character of the ejected electron spectrum all indicate that a Xe nanoplasma core is formed during the x-ray ionization of the cluster. Photoionization heating leads to an electron temperature in the Xe nanoplasmas of around 125 eV; three-body recombination in this nanoplasma leads to a dominance of Xe^{1+} ions in the charge-state distribution.

This work was supported by the U.S. Department of Energy National Nuclear Security Administration under Cooperative agreement DE-FC52-03NA00156, the DOE Office of Basic Energy Sciences, the Welch Foundation

Grant No. F-1626, and by the German Research Foundation DFG Grants No. MO 719/6-1 and No. BO 3/69/2-2.

*Corresponding author.

tditmire@physics.utexas.edu

- [1] T. Ditmire *et al.*, *Phys. Rev. A* **57**, 369 (1998).
- [2] J. W. G. Tisch *et al.*, *Nucl. Instrum. Methods Phys. Res., Sect. B* **205**, 310 (2003).
- [3] C. Bostedt *et al.*, *J. Phys. B* **43**, 194011 (2010).
- [4] H. Thomas *et al.*, *J. Phys. B* **42**, 134018 (2009).
- [5] C. Bostedt *et al.*, *Phys. Rev. Lett.* **100**, 133401 (2008).
- [6] M. Hoener *et al.*, *J. Phys. B* **41**, 181001 (2008).
- [7] H. Wabnitz *et al.*, *Nature (London)* **420**, 482 (2002).
- [8] B. Ziaja *et al.*, *New J. Phys.* **11**, 103012 (2009).
- [9] C. Siedschlag and J. M. Rost, *Phys. Rev. Lett.* **93**, 043402 (2004); B. N. Breizman and A. V. Arefiev, *Plasma Phys. Rep.* **29**, 593 (2003).
- [10] T. Ditmire *et al.*, *Phys. Rev. Lett.* **78**, 2732 (1997).
- [11] J. Krzywinski *et al.* (to be published); P. Emma *et al.*, *Nature Photon.* **4**, 641 (2010).
- [12] O. F. Hagena, *Surf. Sci.* **106**, 101 (1981).
- [13] V. Jonauskas *et al.*, *J. Phys. B* **36**, 4403 (2003).
- [14] R. F. Schmalz, *Phys. Fluids* **29**, 1389 (1986).
- [15] Y. Tamenori *et al.*, *J. Phys. B* **35**, 2799 (2002).
- [16] T. Ditmire *et al.*, *Phys. Rev. A* **53**, 3379 (1996).
- [17] Atomic Calculation of Photoionization Cross-Sections and Asymmetry Parameters, <http://ulisse.elettra.trieste.it/services/elements/WebElements.html>.
- [18] I. H. Suzuki *et al.*, *J. Electron Spectrosc. Relat. Phenom.* **119**, 147 (2001).
- [19] A. M. El Shemi, *Can. J. Phys.* **82**, 811 (2004).